SALT AND PEPPER NOISE FILTERING USING FUZZY LOGIC IN GRAYSCALE IMAGES

Ghazwan Jabbar Ahmed

Electronic Computing Center University of Diyala, Diyala, Iraq

Abstract

Digital image processing plays a pivotal role in various fields, from medical imaging to surveillance systems. However, the acquired images are often susceptible to various types of noise, such in the form of salt and pepper noise, which can severely degrade image quality and hinder subsequent analysis.

In this study, we introduce a fuzzy impulse noise removal algorithm as a potential solution. The efficiency of the suggested algorithms is assessed by comparing their performance to various existing noise removal methods. Objective measurements, including peak signal-to-noise ratio and mean square error, are used to evaluate the results. The findings demonstrate that the proposed algorithms deliver excellent outcomes in noise reduction and image detail preservation across a broad range of noise densities.

--***---

1. INTRODUCTION

Noise can be described as any undesirable signal that contaminates an information-carrying signal It exists to varying degrees in almost all environments. Images often suffer from noise, which can emerge during the image acquisition process, transmission, or reproduction. The removal of noise from images is a crucial task in image processing and represents a significant obstacle to effective image analysis [1-6].

Among the different noise types, impulse noise holds significant prevalence and impact in digital images. This form of noise consists of brief, sporadic instances of "on/off" noise pulses that can introduce disturbances into images during the acquisition stage due to sensor-related issues (such as switching fluctuations or sensor temperature variations), or during transmission caused by channel irregularities (such as interference or atmospheric disruptions)[7-13]. Additionally, impulse noise can emanate from flawed hardware memory positions or synchronization instances discrepancies (similar to errors encountered during analog-to-digital conversion) that occur during the image processing phase [14,15].

and also Salt and Pepper noise, a type of image distortion, adds random black and white pixels to an image, resembling grains of salt and pepper. It can degrade image quality but is commonly encountered in real-world scenarios, requiring effective noise reduction techniques for restoration.[16,17]

Zadeh introduced fuzzy logic in 1965 as a mathematical tool designed to handle uncertainty. It presents a valuable approach for soft computing by incorporating the notion of computing with words and offering a method to address imprecision and information granularity. Within the framework of fuzzy theory, linguistic constructs like "many," "low," "large," "dark," "bright," and others can be effectively represented [18,19]

2. Proposed work

The proposed work comprises two primary stages. Firstly, it involves fuzzy noise detection to identify noisy pixels using suitable fuzzy sets and rules. Each model of impulse noise is treated differently in this stage based on the outcome of the noise identification process. Secondly, the work includes fuzzy noise filtering to recover the pixel values classified as noisy during the identifying noise stage. This filtering is achieved using appropriate fuzzy sets and rules as well.

2.1. Impulse Noise Detection

In numerous scenarios, applying impulse noise filtering without first classifying the noisy and noise-free pixels can lead to image distortion and blurring of edges. As a result, impulse noise detection becomes a crucial preliminary step before proceeding with noise filtering.

Impulse noise is commonly caused by bit errors during data transfer and is characterized by its random and sparse nature. It stays autonomous and uncorrelated with the pixel elements of the image, resulting in some image pixels being noisy while the rest remain noise-free. The impulse noise model can be succinctly described as follows [20-24]:

$$I(x,y) = \begin{cases} n(x,y), & \text{with probability } P \\ O(x,y), & \text{with probability } 1-P \end{cases} \quad \dots (1)$$

In this context, let I(x, y) represent the pixel value of the noisy image, O(x, y) denote the uncorrupted (original) image pixel value, and n(x, y) depict the pixel with impulsive noise at the coordinates (x, y).

In this study, the impulse noise considered is Salt and Pepper noise (SPN). In Salt and Pepper noise, the noisy pixels can take on either the maximum intensity value L_max (gray level 255) or the minimum intensity value L_min (gray level 0). Consequently, the noise appears as white and black spots on the images. As a result, the value of n(x, y) in Equation (1) will be either 255 or 0. If (P) is the total noise density, then the noise density for salt noise and pepper noise will each be (P/2). In some cases, Salt noise and pepper noise could exhibit dissimilar levels of noise densities, denoted as P1 and P2, respectively, and the cumulative noise density will be given by: P = P1 + P2.

When an image is affected by Salt and Pepper noise (SPN), a noisy pixel assumes one of two extreme values, either 0 or 255. Consequently, a pixel having a value of 0 or 255 is classified as a suspected pixel. However, if a suspected pixel closely resembles devoid of noise neighboring pixels, it can be considered as devoid of noise too. Two pixels are deemed similar when their absolute difference in grey value is small but not zero. This is because, in cases where both pixels are noisy, their absolute difference can be equal to zero.

The term "small" to describe the absolute difference can be represented by a fuzzy set called "Small Absolute Difference," with its membership function μ_{small} illustrated in figure (1)
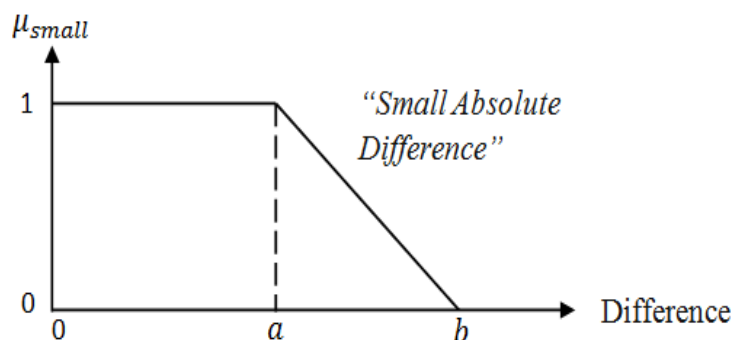

Figure (1): Fuzzy set "*Minor Absolute Deviation*" membership function

The membership function μ for "small"is defined by two predefined parameters, namely a and b, with values a=10 and b=22 as established in [25-30].

The essential steps for detecting Salt and Pepper Noise (SPN) can be outlined as follows:

Consider a neighborhood of size (2K+1)×(2K+1) around a central pixel I(x, y) at position (x, y) in the image I, where K starts with 1. If the value of the central pixel within this window does not match either of the Salt and Pepper noise values (i.e., I(x, y) ≠ 0 or 255), it is identified as a pixel without noise. In any other case, the following steps will be executed:

1. To determine the count of noise-free pixels within the observed window, we utilize the binary matrix M_SP as given in Eq. (3.2) along with the following equation:

$$G_{xy}^d = \sum_{s=-K}^{K} \sum_{t=-K}^{K} M_{SP}(x+s, y+t)$$

… (2)

If ($G_{xy}^d < 1$) , then the

The window size will expand by increasing the value of K. This process is reiterated until the condition is met.($G_{xy}^d \geq 1$) is met.

2. Compute the absolute variances involving the central pixel and its neighboring counterparts within the specified window. as described below:

$$D_{xy} = |I(x+s, y+t) - I(x,y)|, \text{ with } I(x+s, y+t) \neq I(x,y)$$

… (3)

where: $s, t \in \{-K, \dots, +K\}$

3. Find the maximum value in D_{xy} as:

$$m_{xy} = \max(D_{xy})$$

… (4)

4. The membership function μ_{small} is used to determine whether the value of m_{xy} is small as given in the following equation:

$$\mu_{small}(m_{xy}) = \begin{cases} 1, & 1 \leq m_{xy} \leq a \\ \frac{b-m_{xy}}{b-a}, & a \leq m_{xy} \leq b \\ 0, & m_{xy} > b \end{cases}$$

… (5)

5. A fuzzy set named "Noise-Free" is employed to ascertain whether the current pixel I(x, y) can be classified as noise-free. The membership function for this set is derived as follows:

$$\mu_{noisefree}(I(x,y)) = \begin{cases} \mu_{small}(m_{xy}) \text{ if } I(x,y) = (0 \text{ or } 255) \\ 1 \qquad \text{otherwise.} \end{cases}$$

… (6)

2.2. Filtering Impulse Noise

The filtering procedure is applied exclusively to pixels with a membership degree less than one in the Noise-Free fuzzy [22][23] set. (i.e., $\mu_{noisefree}(I(x,y)) < 1$ is considered as a noisy pixel). The filtering window size $(2L+1) \times (2L+1)$ is chosen adaptively according to the output of noise detection stage (i.e., $\mu_{noisefree}$) as follows:

1. Calculate the count of noise-free pixels within that window by:

$$G_{xy}^f = \sum_{s=-L}^{L} \sum_{t=-L}^{L} I(x+s, y+t) \text{ with } \mu_{noisefree}(I(x+s, y+t)) = 1$$

…(7)

2. If ($G_{xy}^f < 1$), Subsequently, the window size will be enlarged by increasing the value of L. This process is reiterated until the specified condition is met ($G_{xy}^f \geq 1$) is met.

In cases where neighboring pixels display similarity or pertain to a notably uniform area, median-based algorithms prove successful in eliminating impulse noise. Nonetheless, in scenarios where pixels are part of regions encompassing edges or intricate image intricacies, the integration of information from other pixels, as represented by their corresponding weights, becomes imperative. Consequently, For every examined filtering window with dimensions (2L+1)×(2L+1), a fuzzy set denoted as 'Similar' is formulated to ascertain the level of similarity for each pixel within the window. This set is then utilized to allocate the suitable weight during the noise detection phase.

Pixels demonstrating akin intensities within the observed filtering window will display a heightened membership degree within the 'Similar' fuzzy set. Likewise, edge pixels, characterized by comparable intensities along the edges, will also exhibit elevated membership degrees. Conversely, pixels affected by noise, deviating in intensities from their adjacent pixels, will manifest lower membership degrees. The 'Similar' fuzzy set is depicted through a Gaussian-shaped membership function denoted as μ_similar, visually represented in figure (2).
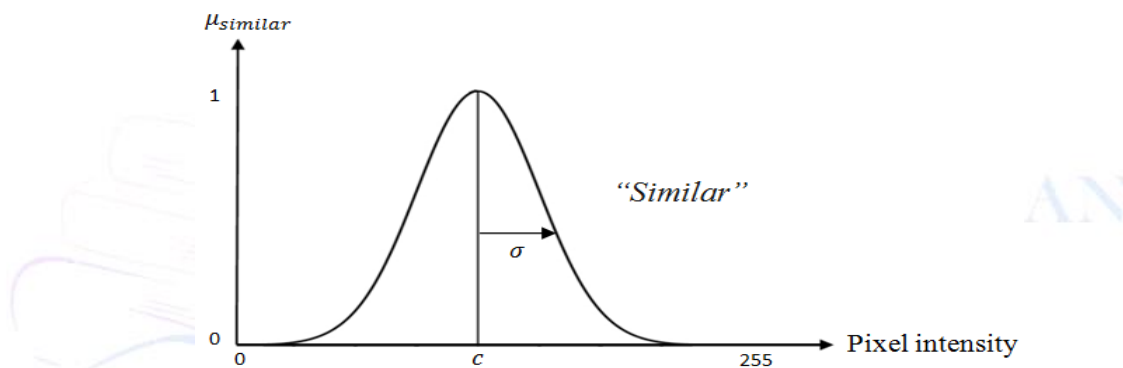

Figure (2) Fuzzy set "Similar" characterized by a membership function resembling μ_similar.

The membership function for the fuzzy set "Similar" is defined through two parameters, namely, c and σ. The parameter c designates the center point of the membership function, where the maximum value is attained. Meanwhile, σ is associated with the distribution width of the membership function. As a result, these parameters are dynamically determined based on the homogeneity within the neighborhood of size (2L+1)×(2L+1), as outlined below:

$$c = \underset{-L\leq s,t\leq L}{\text{mean}}\big(I(x+s, y+t)\big), \text{with } \mu_{noisefree}I(x+s, y+t) = 1 \qquad \text{... (8)}$$

$$\qquad \text{... (9)}$$

$$\sigma = \underset{-L\leq s,t\leq L}{\max}\big(\text{mean}(|I(x+s, y+t) - c|), 0.01\big)$$

The behavior of the membership function $\mu_{similar}$ can be described depending on Eq. (8) and (9) as follows:

1. The extent of the membership function's width will be relatively greater in cases where the observed window belongs to a non-homogeneous region, such as edges or image textures. Conversely, the width of the membership function will decrease as the homogeneity level increases. In rare instances where the noise-free pixels within the observed window have identical values, the value of σ will be zero, potentially leading to an infinite result. To avoid this situation, the Max operation in Eq. (9) is used with a small value (e.g., 0.01) to prevent encountering infinity in Eq. (10).

2. The membership function reaches its maximum level at the average value of noise-free pixels within the observed window.

Consequently, by utilizing the membership function μ_similar, the effectiveness of the filtering process is enhanced. This leads to the removal of noisy pixels while endeavoring to preserve image details to the greatest extent possible. The expression for the membership function μ_similar is as follows:

$$\mu_{similar}(I(x,y)) = e^{-\left(\frac{I(x,y)-c}{2\sigma}\right)^2}$$

… (10)

The final fuzzy weight w_k for each pixel p_k in the observed window of size $(2L+1) \times (2L+1)$ is determined by the following fuzzy rule:

Fuzzy Rule Establishing the degree of fuzzy weighting for p_k:

IF (p_k is *noise-free*) *AND* (p_k is *similar*)

THEN (w_k is *high*)

This rule can be executed through the intersection operation involving two fuzzy sets. Consequently, the validity of the aforementioned rule is achieved by:

$$w_k = \min\{\mu_{noisefree}(p_k), \mu_{similar}(p_k)\}$$ … (11)

In this context, the index k ranges from 1 to (2K+1)^2, enabling the selection of a window element.

Ultimately, the outcome of the fuzzy filtering process for a specific pixel I(x,y) within the analyzed window of dimensions (2K+1)×(2K+1) is denoted as F(x,y). The calculation is performed as follows[6]:

$$F(x,y) = (1-w(x,y)) \times \frac{\sum_{s=-K}^{K}\sum_{t=-K}^{K} I(x+s,y+t).w(x+s,y+t)}{\sum_{s=-K}^{K}\sum_{t=-K}^{K} w(x+s,y+t)} + w(x,y).I(x,y)$$ (12)

Here, $I(x+s,y+t)$ denotes the pixels within the examined window surrounding the central pixel, while $(x+s,y+t)$ signifies the associated weight assigned to each pixel within that window.

3. Experimental Results

In this section, The effectiveness of the suggested grayscale algorithm is assessed through a comparison with the following noise reduction methods: MF[11], HFF[12], AMF[13], FSM[14], and AWTMF[15]. All these methods are applied to the "Parrot" image corrupted with various percentages of Salt and Pepper Noise (SPN).

Table (1) presents the objective quality measurements in terms of PSNR and MSE for the "Parrot" image corrupted with 10%, 30%, and 50% of Salt and Pepper Noise (SPN). The results clearly indicate that the proposed algorithm outperforms the other filtering methods. To further analyze the effect of noise density on the performance, Figure (3) displays the PSNR values of the proposed algorithm and the related methods. These findings are visually confirmed in Figure (4), which showcases the noisy image corrupted with 40% SPN and the corresponding filtered images using all compared methods. Figure (4) illustrates that the proposed algorithm excels in noise suppression and detail preservation.

Figure (3) clearly demonstrates that the proposed algorithm achieves superior results in both low and high noise densities, primarily because of the following main reasons:

1. By employing a robust noise detection scheme

2. The approach involves employing an adaptive window size during both the noise detection stage and noise filtering stage, which is determined dependent on the count of noise-free pixels within the observed window.

3. Incorporating the uncertainty of fuzzy logic in both the noise detection stage and noise filtering stage.

Table (1): The comparative results of the proposed algorithm with different methods in terms of PSNR and MSE

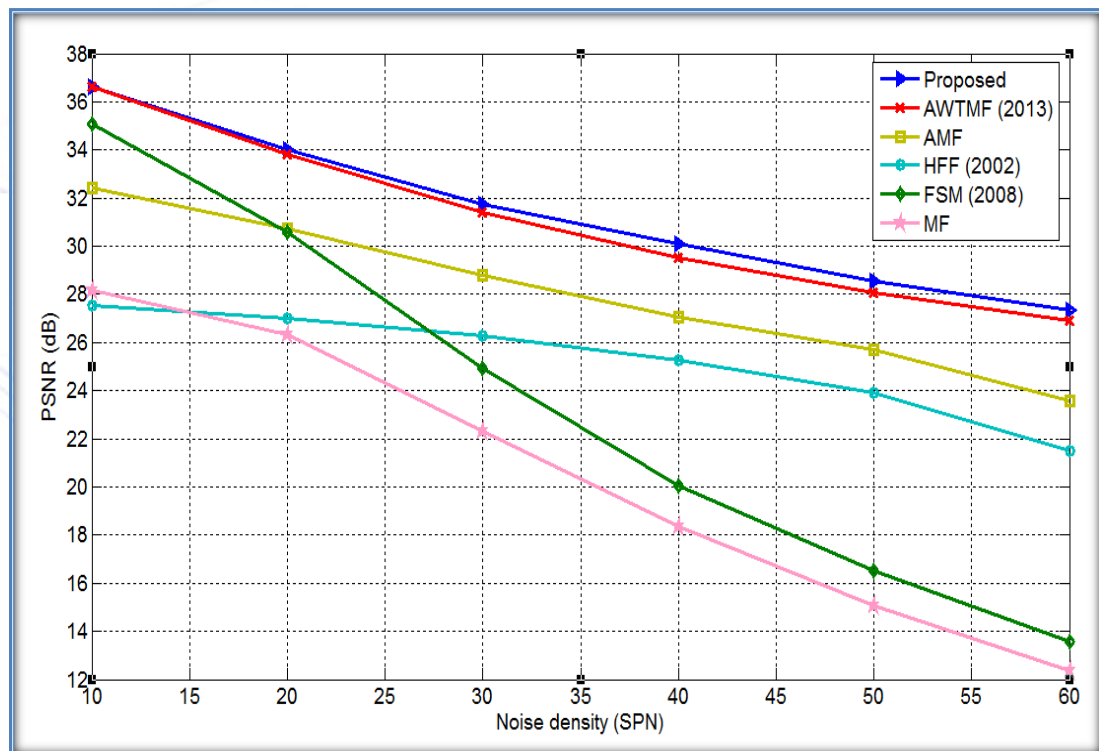| Method	Noise density					
	10%		30%		50%	
	PSNR	MSE ($\times 10^{-2}$)	PSNR	MSE ($\times 10^{-2}$)	PSNR	MSE ($\times 10^{-2}$)
Noisy image	14.76	3.3392	10.75	8.4041	8.50	14.094
MF [11]	28.16	0.1525	22.34	0.5829	15.07	3.1114
HFF [12]	27.54	0.1761	26.29	0.2346	23.90	0.4068
FSM[13]	35.07	0.0311	24.94	0.3201	16.54	2.2132
AMF[14]	32.43	0.0571	28.78	0.1323	25.71	0.2685
AWTMF[15]	36.60	0.0219	31.38	0.0727	28.05	0.1564
Proposed	36.63	0.0217	31.74	0.0669	28.57	0.1388

Figure (3): Comparison chart in PSNR of the proposed algorithm with different methods

Figure (4): The SPN removal results of the "Boats" image are as follows:

(a) Original image

(b) Image tainted by noise contamination 40% SPN (PSNR: 9.46)

(c) Image that has undergone filtering with the utilization of MF (PSNR: 18.34)

(d) Image that has undergone filtering with the utilization of FSM (PSNR: 20.07)

(e) Image that has undergone filtering with the utilization of HFF (PSNR: 25.25)

(f) Image that has undergone filtering with the utilization of AMF (PSNR: 27.05)

(g) Image that has undergone filtering with the utilization of AWTMF (PSNR: 29.54)

(h) Filtered image using the proposed algorithm (PSNR: 30.08).

4. Conclusions

In this study, the following key findings have been concluded:

1. The effectiveness of fuzzy techniques in image noise reduction relies on accurately selecting the appropriate fuzzy sets and fuzzy rules, determining the membership function boundaries with precision, and employing a reliable defuzzification process.

2. The use of an adaptive window size in both the noise detection and noise filtering stages contributed to the superior effectiveness of the suggested algorithms in terms of objective measurements and visual quality, even in cases of high noise density, outperforming other methods.

3. The shape of the membership functions in fuzzy set "Similar," as depicted in figures (2), is dynamically adjusted based on the homogeneity level of the processed window. This characteristic empowers the proposed algorithms to effectively differentiate between image details and noisy pixels, resulting in superior outcomes in relation to the elimination of noise and the preservation of image details.

References

1. Tong-Li He and Jian-Hong Gan, "A new method of removing salt-and-pepper noise basing on grey system model in images," 2010 IEEE International Conference on Intelligent Computing and Intelligent Systems, Xiamen, China, 2010, pp. 574-576, doi: 10.1109/ICICISYS.2010.5658446.

2. R. R. Chand, M. Farik and N. A. Sharma, "Digital Image Processing Using Noise Removal Technique: A Non-Linear Approach," 2022 IEEE Asia-Pacific Conference on Computer Science and Data Engineering (CSDE), Gold Coast, Australia, 2022, pp. 1-5, doi: 10.1109/CSDE56538.2022.10089258.

3. K. Mahboob, S. Khursheed, S. M. Jameel, V. Uddin, S. Shukla and J. K. Pabani, "A Novel Medical Image De-noising Algorithm for Efficient Diagnosis in Smart Health Environment," 2022 Global Conference on Wireless and Optical Technologies (GCWOT), Malaga, Spain, 2022, pp. 1-5, doi: 10.1109/GCWOT53057.2022.9772907.

4. R. R. Chand, M. Farik and N. A. Sharma, "Digital Image Processing Using Noise Removal Technique: A Non-Linear Approach," 2022 IEEE Asia-Pacific Conference on Computer Science and Data Engineering (CSDE), Gold Coast, Australia, 2022, pp. 1-5, doi: 10.1109/CSDE56538.2022.10089258.

5. M. M. Hamid, F. Fathi Hammad and N. Hmad, "Removing the Impulse Noise from Grayscaled and Colored Digital Images Using Fuzzy Image Filtering," 2021 IEEE 1st International Maghreb Meeting of the Conference on Sciences and Techniques of Automatic Control and Computer Engineering MI-STA, 2021, pp. 711-716.

6. M. Rakhshanfar and M. A. Amer, "Low-Frequency Image Noise Removal Using White Noise Filter," 2018 25th IEEE International Conference on Image Processing (ICIP), Athens, Greece, 2018, pp. 3948-3952, doi: 10.1109/ICIP.2018.8451391.

7. M. Shajahan, S. A. M. Aris, S. Usman and N. M. Noor, "IRPMID: Medical XRAY Image Impulse Noise Removal using Partition Aided Median, Interpolation and DWT," 2021 IEEE International Conference on Signal and Image Processing Applications (ICSIPA), Kuala Terengganu, Malaysia, 2021, pp. 105-110, doi: 10.1109/ICSIPA52582.2021.9576773.

8. C. Anjanappa and H. S. Sheshadri, "Development of mathematical morphology filter for medical image impulse noise removal," 2015 International Conference on Emerging Research in Electronics, Computer Science and Technology (ICERECT), Mandya, India, 2015, pp. 311-318, doi: 10.1109/ERECT.2015.7499033.

9. H. K. Aggarwal, S. Tariyal and A. Majumdar, "Compressive hyper-spectral imaging in the presence of impulse noise," 2015 7th Workshop on Hyperspectral Image and Signal Processing: Evolution in Remote Sensing (WHISPERS), Tokyo, Japan, 2015, pp. 1-4, doi: 10.1109/WHISPERS.2015.8075396.

10. T. M. Y. Shiju and A. V. N. Krishna, "A Two-Pass Hybrid Mean and Median Framework for Eliminating Impulse Noise From a Grayscale Image," 2021 2nd International Conference on Advances in Computing, Communication, Embedded and Secure Systems (ACCESS), Ernakulam, India, 2021, pp. 206-210, doi: 10.1109/ACCESS51619.2021.9563285.

11. A. Konieczka, J. Balcerek and A. Dąbrowski, "Method of adaptive pixel averaging for impulse noise reduction in digital images," 2018 Baltic URSI Symposium (URSI), Poznan, Poland, 2018, pp. 221-224, doi: 10.23919/URSI.2018.8406738.

12. Y. Jiang, "A Truncated L1-L2 Total Variational Method for Image Restoration with Impulse Noise," 2022 3rd International Conference on Computer Vision, Image and Deep Learning & International Conference on Computer Engineering and Applications (CVIDL & ICCEA), Changchun, China, 2022, pp. 1-4, doi: 10.1109/CVIDLICCEA56201.2022.9824196.

13. Y. Jiang, "A Truncated L1-L2 Total Variational Method for Image Restoration with Impulse Noise," 2022 3rd International Conference on Computer Vision, Image and Deep Learning & International Conference on Computer Engineering and Applications (CVIDL & ICCEA), Changchun, China, 2022, pp. 1-4, doi: 10.1109/CVIDLICCEA56201.2022.9824196.

14. P. Luo, X. Zhang, Z. Chang and W. Liu, "Research on Salt and Pepper Noise Removal Method Based on Adaptive Fuzzy Median Filter," 2021 IEEE 5th Advanced Information Technology, Electronic and Automation Control Conference (IAEAC), 2021, pp. 387-392

15. G. P. Deepti, M. V. Borker and J. Sivaswamy, "Impulse Noise Removal from Color Images with Hopfield Neural Network and Improved Vector Median Filter," 2008 Sixth Indian Conference on Computer Vision, Graphics & Image Processing, Bhubaneswar, India, 2008, pp. 17-24, doi: 10.1109/ICVGIP.2008.75.

16. X. Lin, L. Tian, Q. Du and C. Qin, "Improved Decision Based Adaptive Threshold Median Filter for Fingerprint Image Salt and Pepper Noise Denoising," 2022 21st International Symposium on Communications and Information Technologies (ISCIT), Xi'an, China, 2022, pp. 233-237, doi: 10.1109/ISCIT55906.2022.9931257.

17. Xiao Kang, Wei Zhu, KeJie Li and Jing Jiang, "A Novel Adaptive Switching Median filter for laser image based on local salt and pepper noise density," 2011 IEEE Power Engineering and Automation Conference, Wuhan, 2011, pp. 38-41, doi: 10.1109/PEAM.2011.6135010.

18. Z. Liu et al., "Fuzzy Logic-Based Adaptive Point Cloud Video Streaming," in IEEE Open Journal of the Computer Society, vol. 1, pp. 121-130, 2020, doi: 10.1109/OJCS.2020.3006205.

19. P. V. S. Reddy, "Generalized Fuzzy Logic with twofold fuzzy set: Learning through Neural Net and Application to Business Intelligence," 2021 International Conference on Fuzzy Theory and Its Applications (iFUZZY), 2021, pp. 1-5.

20. Muna M. Jawad, Ekbal H. Ali, and Adel J. Yousif, A Fuzzy Random Impulse Noise Detection and Reduction Method Based on Noise Density Estimation, International Journal of Scientific & Engineering Research, Volume 5, Issue 3, March 2014, pp. 455-468.

21. H. M. Rehan Afzal, J. Yu and Y. Kang, "Impulse noise removal using fuzzy logics," 2017 32nd Youth Academic Annual Conference of Chinese Association of Automation (YAC), Hefei, China, 2017, pp. 413-418, doi: 10.1109/YAC.2017.7967444.

22. Younghun Song, Yunsang Han and Sangkeun Lee, "Pixel Correlation-based Impulse Noise Reduction," 2011 17th Korea-Japan Joint Workshop on Frontiers of Computer Vision (FCV), Ulsan, 2011, pp. 1-4, doi: 10.1109/FCV.2011.5739722.

23. M. E. Mathew and J. Jeevitha, "An impulse noise cancellation using iterative algorithms," 2014 International Conference on Electronics and Communication Systems (ICECS), Coimbatore, India, 2014, pp. 1-6, doi: 10.1109/ECS.2014.6892579.

24. P. A. Lyakhov, A. S. Voznesensky, E. D. Shalugin, A. R. Orazaev and V. A. Baboshina, "Bilateral and Median Filter Combination for High-Quality Cleaning of Random Impulse Noise in Images," 2022 11th

Mediterranean Conference on Embedded Computing (MECO), Budva, Montenegro, 2022, pp. 1-5, doi: 10.1109/MECO55406.2022.9797149.

25. W. Luo, "Efficient Removal of Impulse Noise from Digital Images", IEEE Transactions Consumer Electronics, vol. (52), No. (2), pp. (523-527), May, 2006.

26. T. Hasuike and H. Katagiri, "A Subjective and Objective Constructing Approach for Reasonable Membership Function Based on Mathematical Programming," 2016 Joint 8th International Conference on Soft Computing and Intelligent Systems (SCIS) and 17th International Symposium on Advanced Intelligent Systems (ISIS), Sapporo, Japan, 2016, pp. 59-64, doi: 10.1109/SCIS-ISIS.2016.0026.

27. P. Biswas and K. K. Halder, "Speckle Noise Reduction from Medical Images Using Gaussian Fuzzy Membership Function," 2021 3rd International Conference on Electrical & Electronic Engineering (ICEEE), Rajshahi, Bangladesh, 2021, pp. 41-44, doi: 10.1109/ICEEE54059.2021.9718944.

28. A. Kumar, T. Sharma, N. K. Verma, P. Sircar and S. Vasikarla, "Detection and Removal of Salt and Pepper Noise by Gaussian Membership Function and Guided Filter," 2019 IEEE Applied Imagery Pattern Recognition Workshop (AIPR), Washington, DC, USA, 2019, pp. 1-9, doi: 10.1109/AIPR47015.2019.9174579.

29. L. Li, P. Cao, J. Yang, D. Zhao and O. R. Zaiane, "A robust fuzzy clustering algorithm using spatial information combined with local membership filtering for brain MR images," 2020 IEEE International Conference on Bioinformatics and Biomedicine (BIBM), Seoul, Korea (South), 2020, pp. 1987-1994, doi: 10.1109/BIBM49941.2020.9313402.

30. M. Kumar and B. Freudenthaler, "Fuzzy Membership Functional Analysis for Nonparametric Deep Models of Image Features," in IEEE Transactions on Fuzzy Systems, vol. 28, no. 12, pp. 3345-3359, Dec. 2020, doi: 10.1109/TFUZZ.2019.2950636.